

Influence of gypsum board type (X or C) on real fire performance of partition assemblies[§]

Samuel L. Manzello*[†], Richard G. Gann, Scott R. Kukuck and David B. Lenhart[‡]

Building and Fire Research Laboratory, National Institute of Standards and Technology, Gaithersburg, MD 20899-8662, U.S.A.

SUMMARY

This paper compares the responses of wall-size partition assemblies, composed of either type X or type C gypsum wallboard panels over steel studs, when each was exposed to an intense room fire. The exposures lasted from the time of ignition to beyond flashover. Heat flux gauges provided time histories of the energy incident on the partitions, while thermocouples provided data on the propagation of heat through the partitions and on the progress toward perforation. Visual and infrared cameras were used to image partition behaviour during the fire exposure. Contraction of the seams of the two types of assemblies occurred under similar thermal conditions on the unexposed surface. However, there were noticeable differences in cracking behaviour. Reduced scale experiments were performed in conjunction with the real-scale fire tests to provide insight into the contraction and cracking behaviour of the different gypsum board types. Results obtained from these experiments are discussed. Copyright © 2006 John Wiley & Sons, Ltd.

Received 22 November 2005; Revised 26 September 2006; Accepted 6 October 2006

KEY WORDS: compartmentation; fire resistance; partitions; wall; heat flux

INTRODUCTION

Traditional fire resistance testing in the United States has been based on ASTM standard E119, 'Standard Test Methods for Fire Tests of Building Construction and Materials' [1]. The analogous international standard is ISO 834 [2]. In these tests, building components are subjected to a constantly increasing furnace temperature intended to represent a standard fire. The components are then rated, with units of time, on their ability to withstand the exposure up to a criterion that is defined as a failure point. This criterion may be either based on the

*Correspondence to: Samuel L. Manzello, National Institute of Standards and Technology (NIST), 100 Bureau Drive, Stop 8662 Bldg. 224, Room A361, Gaithersburg, MD 20899, U.S.A.

[†]E-mail: samuel.manzello@nist.gov

[‡]NRC-NIST Post-Doctoral Fellow.

[§]Official contribution of the National Institute of Standards and Technology. Not subject to copyright in the United States of America.

temperature rise of the unexposed face of the partition assembly or the efflux of hot gases or flames. Generally, the relative ratings of similar construction types are accurate, i.e. if Construction A obtains a higher rating than Construction B in the test, then it is reasonable to expect that it will contain heat, flames and smoke longer in an actual fire. Current model building codes in the United States prescribe specific ratings for construction assemblies.

There are limitations to this approach in providing a known degree of fire safety:

- The test is concluded when the first failure criterion is met. For non-load bearing wall assemblies, this is almost always an excessive temperature on the unexposed face. The more serious fire hazard is the passage of smoke and flames through the partition, and the time to this failure is rarely measured.
- There is no method available to relate the response of the partition under this standard exposure to its response under a different (more realistic) design fire. Most realistic fires do not heat a partition uniformly. Furthermore, real fires can recede, allowing the partition to cool while still in the presence of smoke and flames.

With these issues in mind, the model building codes in the United States (and formal building codes elsewhere) accept the use of performance-based design [3,4], and the fire protection engineering profession is developing first-generation tools to support this practice [5,6]. Under this approach, the designs of construction assemblies are assessed on how they would be expected to perform during selected design fires, with their thermal and radiative exposures. However, it is not feasible, either practically or economically, to test in the full scale all assemblies under a variety of fires, while making quantitative measurements of their responses. A more pragmatic approach would be the use of (perhaps semi-empirical) models capable of accurately predicting the response of construction assemblies to a wide range of fire conditions. These models would draw upon a small subset of full- and reduced-scale tests to yield the predicted response.

NIST has embarked on a course to provide a methodology for the inclusion of quantitative fire resistance of partitions in performance-based design of buildings. The research involves obtaining real-scale experimental data, modelling the behaviour of partitions as they are driven to failure by the fire and developing recommendations for obtaining as many of the needed model parameters as possible from modifications to standard fire resistance tests such as ASTM E119 and ISO 834.

This paper develops further understanding of the phenomena that govern the performance of a common wall assembly: a non-load-bearing wall of gypsum panels attached with screws to steel studs. Two different types of gypsum wall board assemblies were exposed to actual fire exposures. Reduced scale experiments were performed in conjunction with the real-scale fire tests to provide insight into the contraction and cracking behaviour of the different gypsum board types. The collected data is being used to develop and validate a model capable of accurately predicting the response of partition assemblies to a wide range of fire conditions.

EXPERIMENTAL DESCRIPTION

Two non-load bearing walls consisting of gypsum panels attached to steel studs were constructed for fire testing. Figures 1 and 2 display exposed face and unexposed face

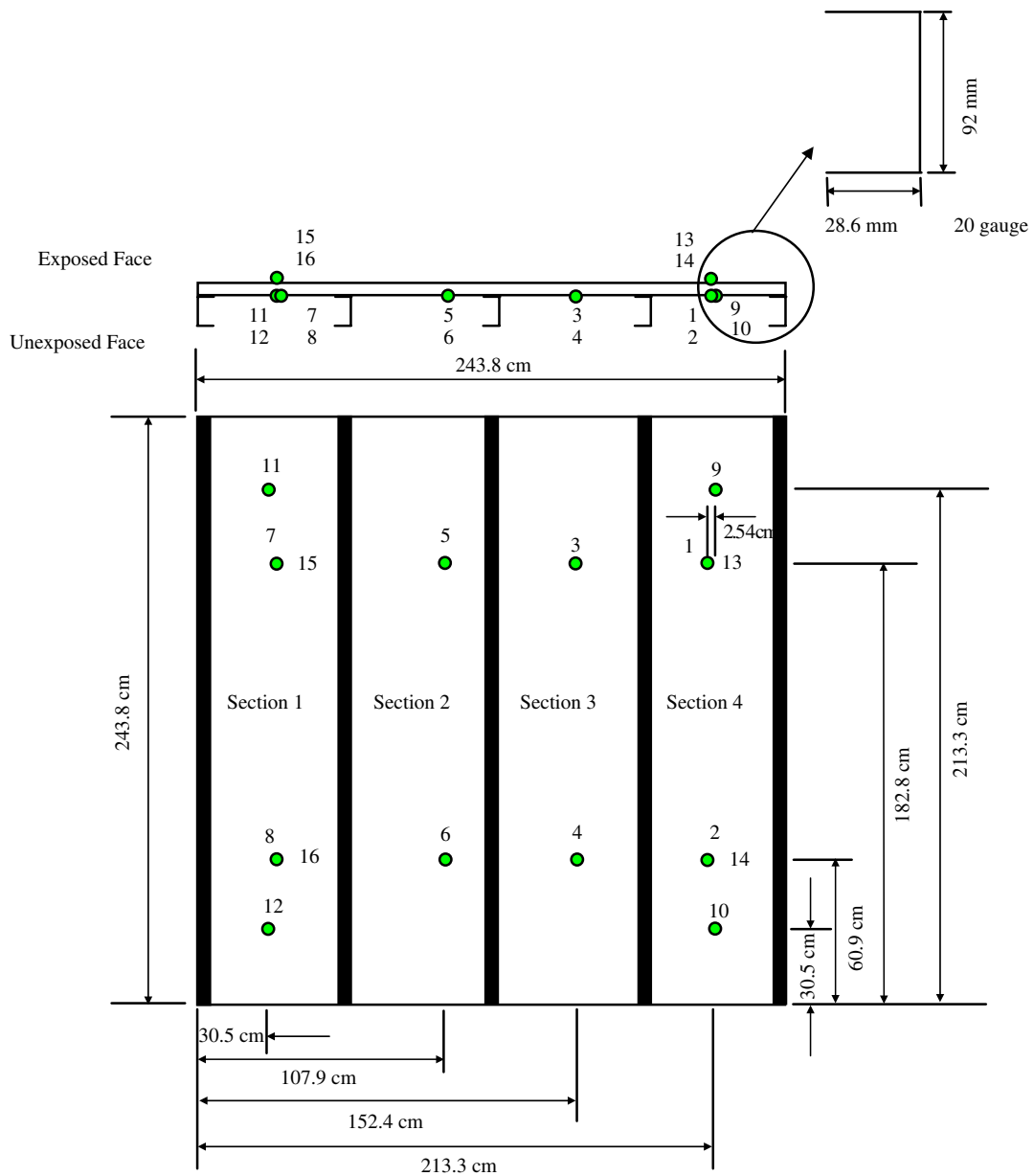


Figure 2. Drawing of Assembly One and Assembly Two, showing the location of the unexposed face temperature measurements.

Test measurements

Temperatures were obtained using type K thermocouples (22 gauge) attached to both sides of the gypsum panels. Bare thermocouples were used on the exposed face. Thermocouples

at the unexposed face were placed under insulating pads in order to compare these measurements to the failure modes of the standard. To model the unexposed surface temperatures accurately, one must account for the thermal resistance induced by the pads [11]. The locations of the thermocouples were identical for the two assemblies and are displayed in Figure 2.

Four Schmidt–Boelter water-cooled total heat flux gauges were used to measure the heat flux incident on the partitions. The position of all four gauges (designated as HF1, HF2, HF3, and HF4) was the same for both partition assemblies tested (see Figure 1). Two gauges were mounted flush to the exposed face of the gypsum panels, and two gauges were mounted flush to the column adjacent to the other vertically mounted gypsum panel. The gauges were mounted on the column in order to have one of the gypsum panels free from the holes necessary for gauge mounting. For the gauges mounted on the gypsum panel, a custom bracket was constructed to support the weight of the gauges and water lines.

To mitigate water condensation on the gauge surface, each gauge was water cooled to $75 \pm 5^\circ\text{C}$, which is well above the dew point. Since soot deposition on the gauge surface was not desired, each gauge was purged with nitrogen for 3 s, every 120 s, during the test. The purge signal was apparent in the flux data and was subsequently removed from the temporal heat flux trace. Although each gauge was provided with a calibration from the manufacturer, the gauges were re-calibrated at NIST at 75°C , prior to the test series. The response of the gauges was re-calibrated upon completion of the test series. The calibrations before and after the test series agreed to within the uncertainty of the calibration procedure.

The unexposed face of each partition assembly was imaged using a standard (visual) video camera with a framing rate of 30 frames/s. In addition, an infrared camera was used to image the unexposed face, also at 30 frames/s. Prior to each test, photographs were taken at 2048×1024 pixel resolution of both the exposed and unexposed faces using a digital camera fitted with a zoom lens. Another series of photographs were taken of both faces upon completion of each test.

Compartment design and fire loading

The size of the compartment for the fire experiments was 10.7 m long \times 7.0 m wide \times 3.4 m high. A schematic of the compartment is displayed in Figure 3(a). A 2.44 m \times 2.44 m opening was constructed on the lower 7.0 m side of the compartment so that each partition assembly could be mounted easily for each fire test. A photograph of the fire compartment is shown in Figure 3(b).

The compartment was constructed to simulate a common office space that would be found in a commercial building. Accordingly, the combustibles within the compartment consisted of three workstations for each of the fire exposures reported here. The fires were ignited using a spray burner (see Figure 3(a)). The fire exposures had peak heat release rates (HRR) of 12.0 MW at 825 s after ignition and 10.5 MW at 912 s after ignition for Assembly One and Assembly Two, respectively. The total burn time for each fire was approximately 45 min. Extensive details of the compartment and the combustibles within the compartment are available elsewhere [12].

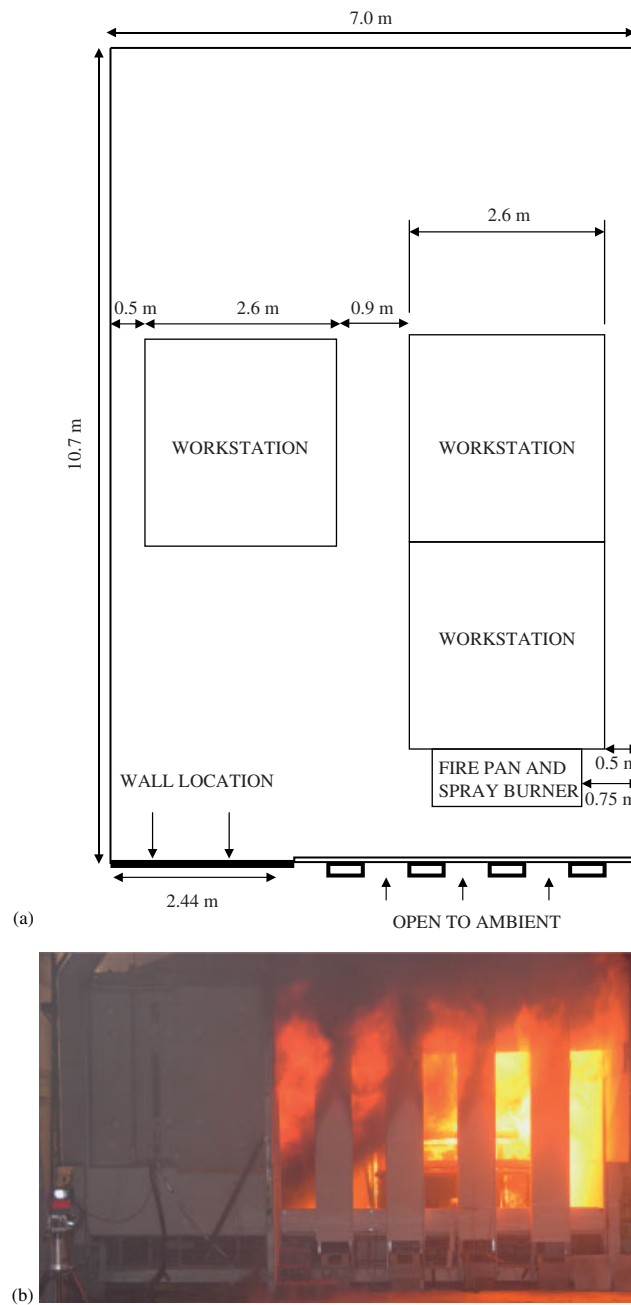


Figure 3. (a) Schematic of compartment where Assembly One and Assembly Two were installed; and (b) photograph of the compartment where Assembly One and Assembly Two were installed.

RESULTS AND DISCUSSION

Type X gypsum board—Assembly One

Figure 4(a) is a picture of Assembly One taken immediately after the fire test. The paper on the exposed face had burned off, and significant cracking occurred on both gypsum panels. It is well known that, upon heating, gypsum panels contract due to dehydration [11]. The opening along the seams of the two gypsum panels due to contraction is clearly visible. Cracks were observed to occur at the screw locations. The formation of cracks at the screw locations was expected since it is these locations that experience the greatest mechanical stress. In addition, a series of transverse cracks was observed to form in both gypsum panels. Both gypsum panels were intact upon completion of the fire test. Overnight, during the cooling process, the gypsum board began to fall apart, resulting in the missing sections. (Entry was not permitted into the fire compartment until the next day due to safety concerns.)

The temporal evolution of openings and crack propagation was analysed using the IR camera and standard video camera and was observed to occur in the following order:

- (1) Opening at the joint between the two vertically mounted gypsum panels (initiation at 1243 s). It is apparent that the tape and spackling compound degraded, and the contraction of the two gypsum panels resulted in opening at the joint.

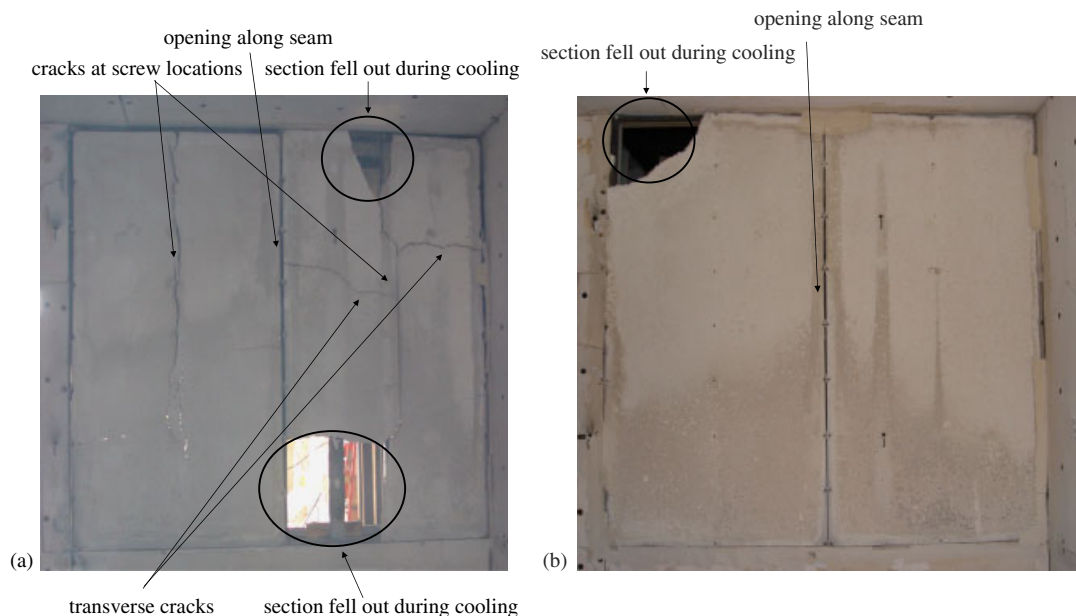


Figure 4. Digital pictures of the exposed face of: (a) Assembly One; and (b) Assembly Two, immediately after their respective fire exposure.

- (2) Cracks at the screw locations along studs (initiation at $t = 1550$ s, first visible in the upper portion of Section 3).
- (3) Transverse cracks (initiation in Section 2 at $t = 2200$ s). The transverse cracks that formed on the exposed face, corresponding to Sections 3 and 4 on the unexposed face, were not visible on the unexposed face during the fire exposure.

To gain insights into the conditions for crack and opening production, it is necessary to understand the thermal load imparted by the fire. Plotted in Figure 5(a) are exposed face temperature measurements during the test for Assembly One. It is estimated that the combined uncertainty for the temperature measurements is $\pm 10^\circ\text{C}$ for temperatures lower than 200°C and $\pm 30^\circ\text{C}$ for temperatures higher than 200°C . The temperatures measured at thermocouple 13 were higher than those measured at locations 14, 15, and 16. Figure 5(b) displays the temporal evolution of measured total heat flux as function of time for the four positions on the exposed face of Assembly One. The total heat flux increased most rapidly at location HF-1 and reached a value of 200 kW/m^2 at 1300 s after ignition. The total heat flux was similar in magnitude at locations HF-2, HF-3, and HF-4. These trends were in agreement with the exposed face temperature measurements.

The unexposed face temperature measurements are reported in Figure 6 for Assembly One. This assembly failed the ASTM E119 temperature rise criterion 1100 s after ignition. The temperature rise on the unexposed face is observed to be a function of location. Based on temperature and total heat flux measurements on the exposed face, it is not surprising that the unexposed face temperatures rose most quickly at thermocouple locations 1, 3 and 9. These measurements were taken on surfaces not directly exposed to the large heat fluxes of the fire exposure and were also taken from underneath the insulating pad. It is estimated that the uncertainty in these measurements is approximately $\pm 10^\circ\text{C}$.

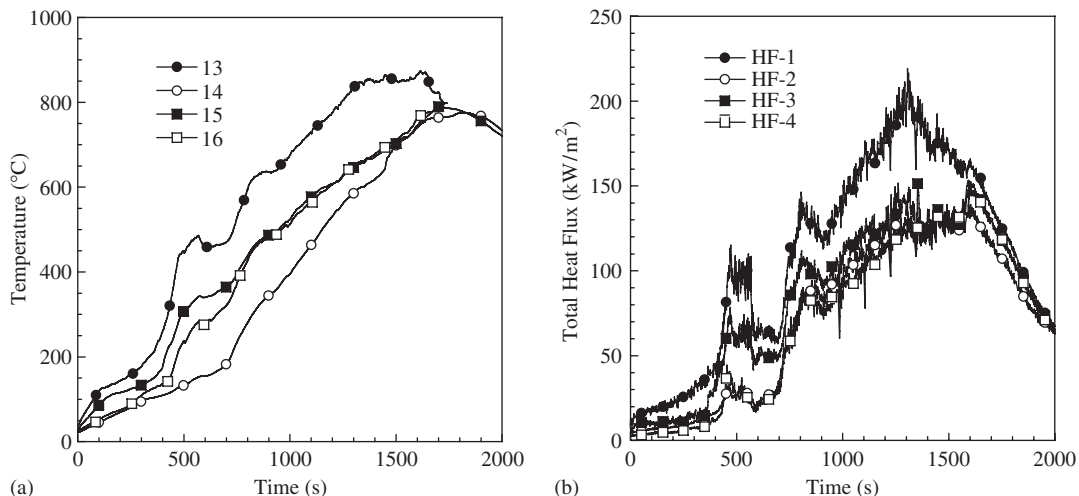


Figure 5. (a) Temporal evolution of the exposed face temperature measurements for Assembly One as a function of location; and (b) temporal evolution of the total heat flux measurements for Assembly One as a function of location.

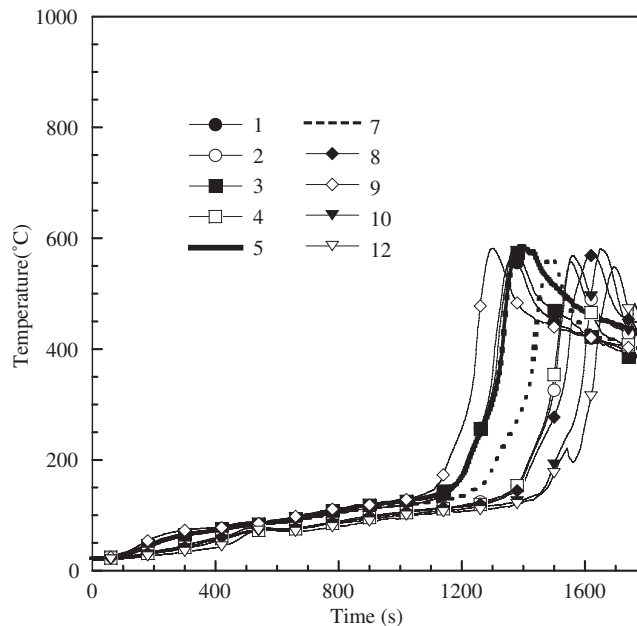


Figure 6. Temporal evolution of the unexposed face temperature measurements for Assembly One as a function of location.

Type C gypsum board—Assembly Two

There were distinct differences between the behaviour of the assemblies with the two types of gypsum board. An image of the exposed face of Assembly Two is displayed in Figure 4(b). The paper on the exposed face burned off, and the opening along the seams of the two gypsum panels due to contraction is clearly visible. No cracks were observed at the screw locations, nor were transverse cracks observed. The opening at the joint between the two vertically mounted gypsum panels was observed to occur at 1370 s after ignition. As was observed for Assembly One, both gypsum panels were intact upon completion of the fire test, i.e. the opening in the picture did not occur during the fire exposure, but during the overnight cool down process.

The exposed face temperature measurements for Assembly Two are displayed in Figure 7(a). Similar to the data obtained for Assembly One, the hottest location was clearly on the gypsum panel fitted with thermocouple 13. Thermocouple 14 is not shown in this figure, as it failed at the beginning of the test. Total heat flux data collected during the fire exposure for Assembly Two are displayed in Figure 7(b). At location HF-1, the total heat flux increased rapidly to a peak value of 180 kW/m^2 at 1300 s. At this location (HF-1), total heat flux was sustained at more than 150 kW/m^2 for over 500 s.

The outside face temperatures of the unexposed board for Assembly Two are displayed in Figure 8. The insulation failure criterion was reached 1250 s after ignition. Similar to Assembly One, the timeline of events from the videographic records agreed with the magnitude of the unexposed face temperature measurements.

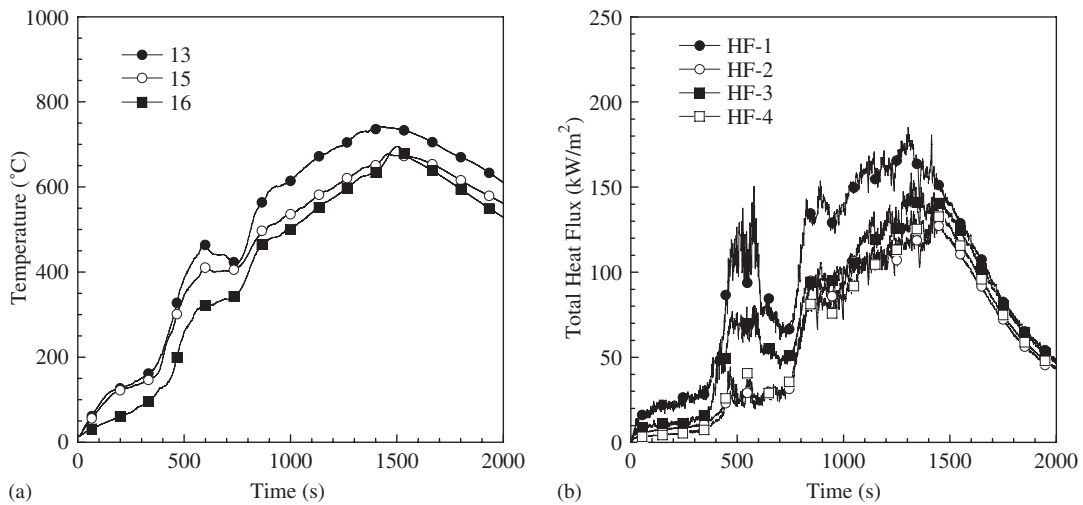


Figure 7. (a) Temporal evolution of the exposed face temperature measurements for Assembly Two as a function of location; and (b) temporal evolution of the total heat flux measurements for Assembly Two as a function of location.

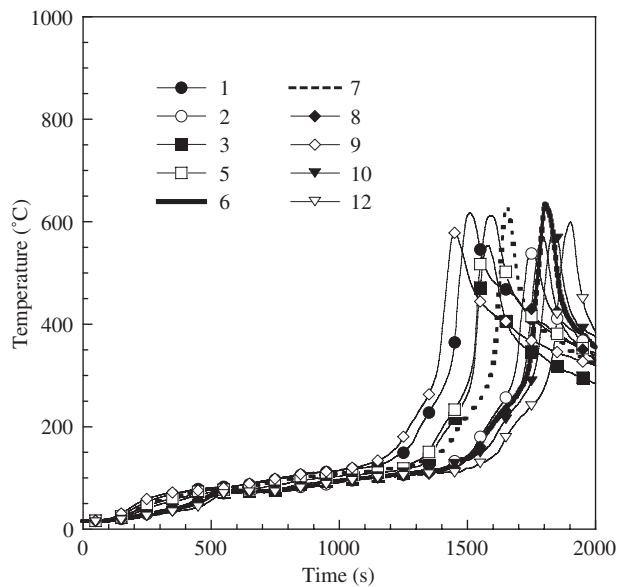


Figure 8. Temporal evolution of the unexposed face temperature measurements for Assembly Two as a function of location.

Contraction and cracking of gypsum board

For a performance-based design approach, it is important to know when wall assemblies collapse and when their effectiveness as a smoke and flame barrier is compromised due to

gypsum board shrinkage and cracking. While many investigators have recognized the importance of modelling the response of both wood- and steel-framed partition assemblies to fire exposure [11,13–18], such models can generally only predict the behaviour of the partition up to the point of insulation failure, as specified under ASTM E119 and ISO 834. The standard insulation criterion is itself of marginal value in assessing fire hazard. Auto-ignition of combustibles on the far side of the wall requires both much higher temperatures and good thermal contact between the wall and the combustibles. Information on the additional failures modes are needed for a model to estimate how long a partition can contain flames and smoke. The model of Takeda [13] has begun to address some of this by incorporating the contraction of gypsum board on the exposed face at the seams in his model.

In order to compare the performance of the two types of assemblies, the total heat flux and gypsum board temperature profiles were analysed at the time when the openings of the gypsum board at the seams were observed on the unexposed face (from camera IR view). Figure 9 displays the average total heat flux measured for Assembly One and Assembly Two. The average total heat flux profiles were obtained by averaging the spatially resolved heat flux data as a function of time. Overall, the two profiles are very similar, which demonstrates that the thermal load due to the fire exposure was similar.

For Assembly One, the average gypsum board temperature (average based on exposed and unexposed face temperature measurement) and the average total heat flux were 417°C and 140 kW/m^2 , respectively, when contraction of the gypsum board at the seams were observed on the unexposed face. For Assembly Two, the average gypsum board temperature (exposed and unexposed face) and the average total heat flux were 412°C and 143 kW/m^2 , respectively, when contraction of the gypsum board at the seams were observed on the unexposed face.

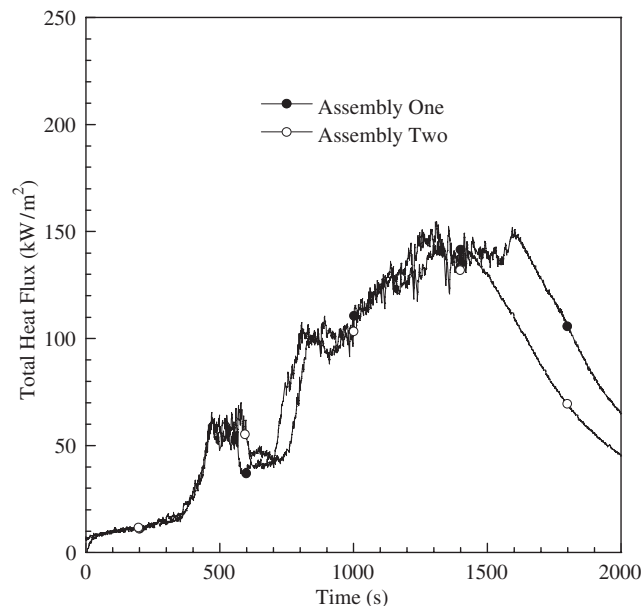


Figure 9. Temporal variation of the average total heat flux measured for Assembly One and Assembly Two.

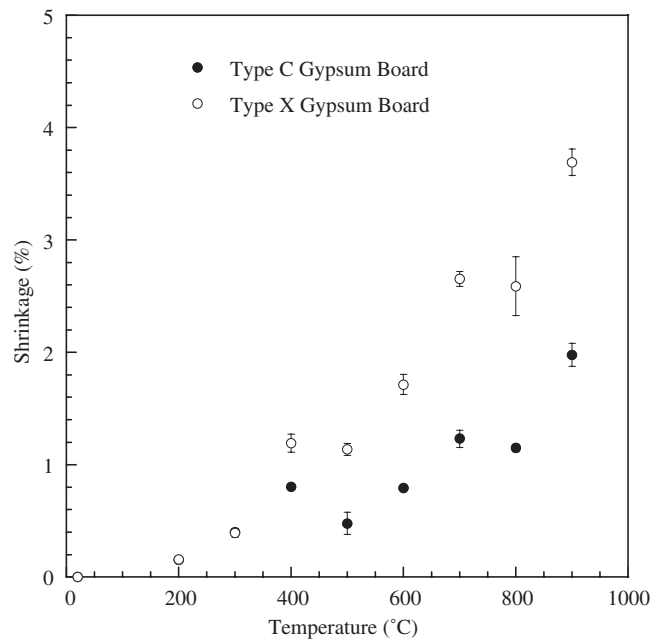


Figure 10. Measured gypsum board contraction as a function of temperature for type X and type C gypsum board samples. Contraction measurements were the same for the type X and type C boards at 200 and 300°C.

In the same series of experiments, Manzello *et al.* [19] exposed an assembly identical to Assembly One (designated Assembly One in that paper) to a different fire exposure. For that test, the average gypsum board temperatures (exposed and unexposed face) and exposed face total heat flux measured were 416°C and 148 kW/m², when contraction of the gypsum board at the seams were observed on the unexposed face. Since these values are virtually the same as those observed for Assembly One, they suggest that the contraction leading to the seam opening is a relatively fast process and is not particularly dependent on the earlier thermal history.

Additional measurements were performed under reduced scale to provide further insights into gypsum board contraction. Triplicate samples of 15.9 mm thick Type X gypsum board (USG) and Type C gypsum board (USG) were cut into 50 mm × 152 mm rectangles from single sheets of each type and inserted into an oven. A series of scoping experiments was conducted in which samples were heated to a selected temperature and their mass measured as a function of time. Further weight loss was insignificant after about 3 h in the oven.

Fresh samples were then heated in 100°C steps. At the end of each step (3 h), a sample was removed from the oven, its width was measured using high precision calipers ($\frac{1}{100}$ mm resolution), and the sample was returned to the oven within 30 s. The results of these measurements are displayed in Figure 10 (as well as Tables I and II). The error bars represent the standard deviation in the measurement of three samples at each temperature.

The linear shrinkage of the gypsum board samples was clearly a function of temperature and gypsum board type. For temperatures below 400°C, the degrees of shrinkage of the two types of gypsum board were not significantly different. As the temperature was increased, the degree of

Table I. Contraction data for type X board.

Heating temperature (°C)	% Shrinkage from the initial sample dimension	
	Heating only	Heating and cooling to 120°C
200	0.15	0.22
300	0.39	0.52
400	1.19	1.50
500	1.13	1.56
600	1.71	2.29
700	2.65	3.43
800	2.58	3.50
900	3.69	4.67

Table II. Contraction data for type C board.

Heating temperature (°C)	% Shrinkage from the initial sample dimension	
	Heating only	Heating and cooling to 120°C
200	0.15	0.20
300	0.39	0.53
400	0.80	1.17
500	0.50	1.0
600	0.78	1.31
700	1.23	1.72
800	1.14	1.98
900	1.97	3.08

shrinkage increased dramatically for the type X gypsum board compared to the type C gypsum board. For example, at 600°C, the degree of shrinkage of type X board was more than twice that of type C board.

Takeda [13] has measured contraction of 50 mm × 200 mm × 12.7 mm thick samples of type X gypsum board as a function of temperature in an oven up to 700°C. The shrinkage of the gypsum board increased, reaching 1.7% at 700°C. This is significantly lower than the value measured here and indicates a difference in the boards tested, an effect of the dimensions of the boards, or a difference in the heating protocol.

In addition to gypsum board contraction measurements, we measured the mass loss of 50 mm × 152 mm × 15.9 mm thick gypsum board samples of both types as a function of temperature. The mass loss of the gypsum board samples was obtained using a load cell (resolution of 5 mg—for reference the initial gypsum board samples had a mass of 80 g (type X) to 100 g (type C), and the results of these measurements are shown in Figure 11. Three replicate experiments were performed at each temperature, with the error bars representing the standard deviation in the measurements at each temperature.

A significant amount of mass was lost for both gypsum board types for temperatures up to 400°C. This was expected since the core of type X gypsum board is known to contain approximately 21% by mass of chemically bound water. For type X gypsum board, the

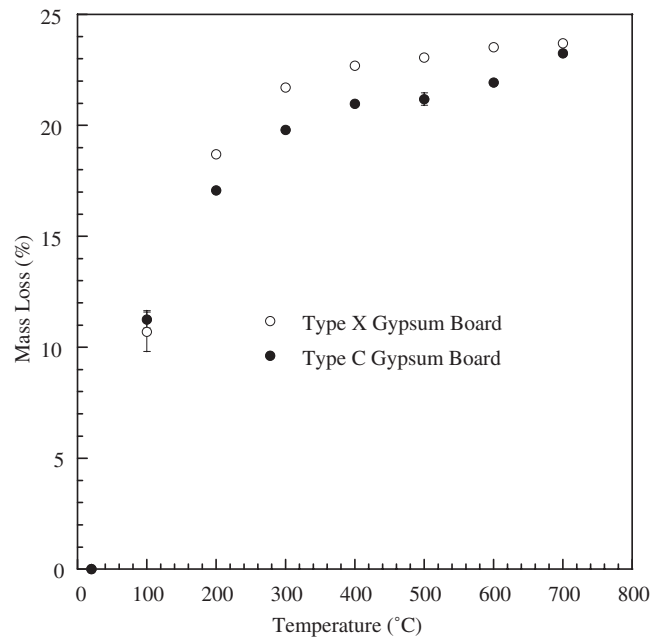


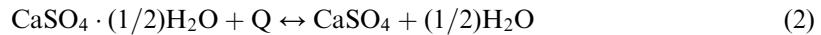
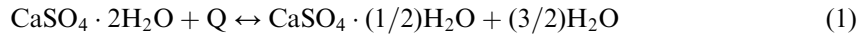
Figure 11. Measured mass loss of type X and type C gypsum board samples as a function of temperature.

21% was reached at about this temperature, but there was further mass loss up to about 600°C. The type C gypsum board reached 21% mass loss at about 400°C, stabilized, and then lost additional mass up to 700°C. At 700°C, all six samples had lost about 23% of their mass.

Understanding of this mass loss behaviour and the difference between the two types of gypsum board lies in the details of the composition of the two materials. ASTM C1396/C1396M [20] contains specifications for type X gypsum board. Type X gypsum board contains a fibrous glass mesh which is designed to hold the gypsum board in place after the dehydration reactions have occurred. There is no ASTM standard for type C gypsum board. As a result, type C gypsum board is generally manufacturer-specific. It is common practice to include other additives, in addition to a fibrous glass mesh, with vermiculite being commonly used. As the gypsum board is heated and the dehydration reactions occur, resulting in contraction of the gypsum, the vermiculite expands. The combination of the fibrous glass mesh and expanding vermiculite act to mitigate contraction and ultimately reduce cracking in the gypsum board. The present experiments, both real-scale and reduced-scale, confirm this behaviour.

The core material of gypsum board is a porous solid composed primarily of calcium sulphate dihydrate ($\text{CaSO}_4 \cdot 2\text{H}_2\text{O}$), a naturally occurring mineral in which two water molecules are chemically bound for every one calcium sulphate molecule within the crystal matrix. The presence of the water molecules is a key feature in establishing the fire resistance properties of gypsum. When heated, crystalline gypsum dihydrates and water is liberated, typically in two

separate, reversible chemical reactions [14]



Both of these dehydration reactions are endothermic and generally occur at temperatures between 125 and 225°C. At a temperature around 400°C, a third, exothermic reaction occurs, in which the molecular structure of the soluble crystal reorganizes itself into a lower insoluble energy state (hexagonal to orthorhombic [21])



These reactions can also be observed in the differential scanning calorimetry (DSC) traces presented in Figures 12 and 13 for type X and type C gypsum board, respectively [22]. These DSC specific heat measurements were taken following the procedure outlined in ASTM E 1269-

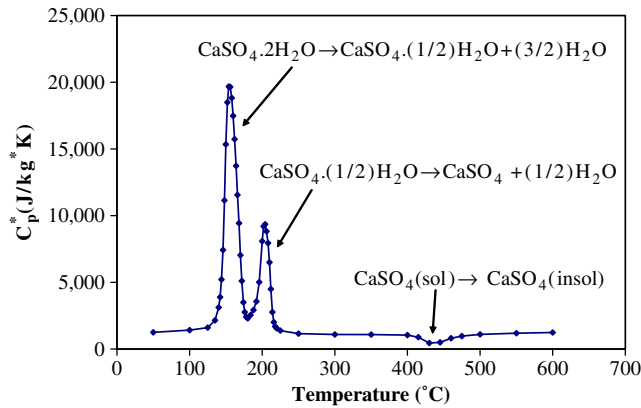


Figure 12. Apparent specific heat of type X gypsum board.

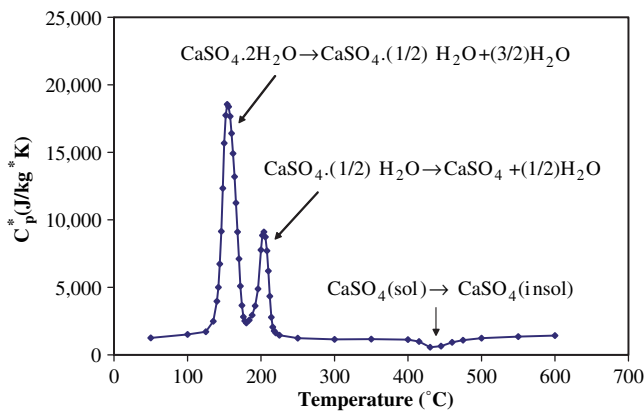


Figure 13. Apparent specific heat of type C gypsum board.

2001 [23] at a scanning rate of 20°C/min. To accommodate the gas generation incurred from dehydration, the sample, reference and standard measurements utilized pans that were sealed except for a 50 µm pinhole in the lid. The curves shown represent the average results of three replicate measurements. The first two reactions, at approximately 150 and 200°C, are strongly endothermic while the third reaction is slightly exothermic, as discussed above.

The DSC traces show that significant reaction, and thus water loss, is completed by the time the board reaches 250°C. While the oven tests show some slight mass loss above 250°C (on the order of 2 to 3%), we attribute this to other ingredients contained in the board. These ingredients include the paper backing, which will pyrolyze at temperatures greater than 250°C, as well as other filler materials contained within the core; e.g. starches, polymers, etc. that can also pyrolyze or vaporize.

When cracks were observed at the screw locations for Assembly One, the average temperature of the gypsum board (exposed and unexposed face) was 600°C and the average exposed face heat flux was 137 kW/m². For the identical assembly but different fire exposure [19] mentioned above, the average gypsum board temperatures (exposed and unexposed face) and exposed face total heat flux measured were similar: 589°C and 115 kW/m², when cracks were observed at the screw locations.

It is known that the screw locations are the points where the greatest mechanical stress exists, due to screw penetration. The data from the real-scale experiments showed that as the average temperature of type X gypsum board approached 600°C, significant cracking occurred. The type

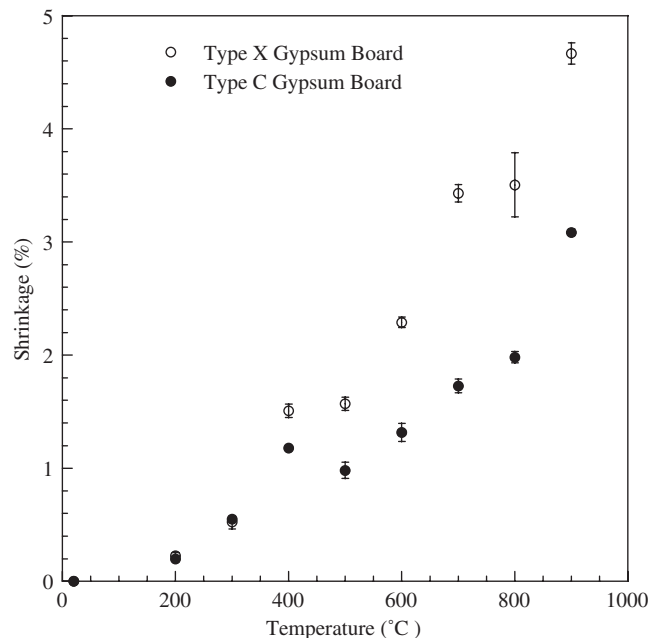


Figure 14. Measured gypsum board contraction as a function of temperature for type X and type C gypsum board samples. For these measurements, the samples were heated to their respective temperatures, samples were then removed and inserted into oven held at 120°C. The contraction measurements were performed when samples equilibrated to 120°C.

C gypsum board for Assembly Two also reached 600°C, but cracks at the screw locations did not materialize throughout the test. It is suggested that these cracks formed because the type X gypsum board contracted to such a degree that the gypsum board pulled away from screws. The type C gypsum board contraction at 700°C was equivalent to type X gypsum board contraction at only 400°C. No cracks were observed for type X board at 400°C. Thus, the lack of cracking at the screw locations in the type C board may be due to the lower degree of contraction at the screw locations.

The transverse cracks that were observed to form in Assembly One occurred after the fire reached its peak heat release rate and was in the decay phase. At this time, the gypsum board was cooling as well. It was hypothesized that as the gypsum board cools, it may continue to contract. To test this supposition, gypsum board samples were heated to one of the several prescribed temperatures for 3 h, then transferred to another oven at 120°C, where it remained for another 3 h. The contraction of the sample from the initial dimension was then measured. Figure 14 displays the result of these experiments. Especially for temperatures at or above 400°C, the contraction is considerably larger than the contraction measured when the gypsum board samples are at the elevated temperatures shown in Figure 10. This is further shown in Tables I and II.

CONCLUSION

Both full-scale and reduced-scale experiments were performed to gain insight into the behaviour of type X and type C gypsum board partitions, especially the cracking that could lead to wall perforation and the passage of smoke and flames into adjacent compartments. The opening of the seam between adjacent panel occurred at similar board temperatures and incident total heat fluxes on the exposed face. The type X panels showed cracking at the mounting screws and transverse cracking at longer times and higher temperatures; the type C panels did not. Reduced scale experiments replicated the shrinkage, suggesting that such (less costly) measurements might be a predictor of crack formation at seams and mounting screws. The reduced shrinkage of type C board, relative to type X board, at higher temperatures is a plausible explanation for the non-formation of cracks in the real-scale test.

For a performance-based design approach, it is important to know when wall assemblies collapse and when their effectiveness as a smoke and flame barrier is compromised due to gypsum board shrinkage and cracking. This work clearly demonstrates that in order to model the failure of partition assemblies, it is important to incorporate gypsum board contraction and crack formation into future models.

ACKNOWLEDGEMENTS

The authors are indebted to the staff of the Large Fire Laboratory (LFL) at NIST for assistance in the experiments. In particular, we are grateful to Mr Alexander Maranghides, Mr Jay McElroy, Mr Lauren DeLauter, Mr Ed Hnetovsky, Mr Gale Miller, and Mr Marco Fernandez.

REFERENCES

1. ASTM E119-00a. *Test Method for Fire Resistance Tests of Building Construction and Materials*. ASTM International: West Conshohocken, PA, 2000.

2. ISO 834 Parts 1 through 9. *Fire Resistance Tests—Elements of Building Construction*. International Organization for Standardization: Geneva, Switzerland.
3. NFPA 5000. *Building Construction and Safety Code* (2003 edn). National Fire Protection Association: Quincy, MA, 2003.
4. *International Building Code (IBC)* (2003 edn). International Code Council: Falls Church, VA, 2003.
5. Bukowski RW. Prediction of the structural fire performance of buildings. *8th Fire and Materials Conference*, San Francisco, CA, 2003.
6. CIB-W14. *Rational Fire Safety Engineering Approach to Fire Resistance of Buildings, Publication 269*. International Council for Research and Innovation in Building Construction: Rotterdam, Netherlands, 2001.
7. ASTM C754-00. *Standard Specification for Installation of Steel Framing Members to Receive Screw-Attached Gypsum Panel Products*. ASTM International: West Conshohocken, PA, 2000.
8. ASTM C840-03. *Standard Specification for Application of Finishing of Gypsum Board*. ASTM International: West Conshohocken, PA, 2003.
9. ASTM C645-00. *Standard Specification for Nonstructural Steel Framing Members*. ASTM International: West Conshohocken, PA, 2000.
10. ASTM C1002-01. *Standard Specification for Steel-Piercing Tapping Screws for the Application of Gypsum Panel Products or Metal Plaster Bases to Wood or Steel Studs*. ASTM International: West Conshohocken, PA, 2001.
11. Sultan MA. A model for predicting heat transfer through noninsulated unloaded steel-stud gypsum board wall assemblies exposed to fire. *Fire Technology* 1996; **32**:239–259.
12. Hamins A, Maranghides A, McGrattan K, Ohlemiller T, Anleitner R. *Federal Building and Fire Safety Investigation of the World Trade Center Disaster: Experiments and Modeling of the Multiple Workstations Burning in a Compartment*. NIST NCSTAR 1-5E, National Institute of Standards and Technology: Gaithersburg, MD, 2005.
13. Takeda H. A model to predict the fire resistance of non-load bearing wood-stud walls. *Fire and Materials* 2003; **27**:19–39.
14. Takeda H, Mehaffey JR, Wall 2D: a model for predicting heat transfer through wood-stud walls exposed to fire. *Fire and Materials* 1998; **22**:133–140.
15. Richardson LR, Batista M. Revisiting the component additive method for light-frame walls protected by gypsum board. *Fire and Materials* 1997; **21**:107–114.
16. Axenenko O, Thorpe G. The modeling of dehydration and stress analysis of gypsum plasterboards exposed to fire. *Computational Material Science* 1996; **6**:281–294.
17. Mehaffey JR, Cuerrier P, Carisse G. A model for predicting heat transfer through gypsum-board/wood-stud walls exposed to fire. *Fire and Materials* 1994; **18**:297–305.
18. Fredlund B. Modeling of heat transfer and mass transfer in wood structures during fire. *Fire Safety Journal* 1993; **20**:39.
19. Manzello SL, Gann RG, Kukuck SR, Prasad K, Jones WW. Real fire performance of partition assemblies. *Fire and Materials* 2005; **29**:351–366.
20. ASTM C1396/C1396M-01. *Standard Specification for Gypsum Board*. ASTM International: West Conshohocken, PA, 2001.
21. Ramachandran VS, Paroli RM, Beaudoin JJ, Delgado AH. *Handbook of Thermal analysis of Construction Materials*. Noyes Publication, William Andrew Publishing: Norwich, NY, 2003.
22. Carino NJ, Starnes MA, Gross JL, Yang JC, Kukuck S, Prasad KR, Bukowski RW. *Federal Building and Fire Safety Investigation of the World Trade Center Disaster: Passive Fire Protection*. NIST NCSTAR 1-6A, National Institute of Standards and Technology: Gaithersburg, MD, 2005.
23. ASTM E 1269-2001. *Standard Method for Determining Specific Heat Capacity by Differential Scanning Calorimetry*. American Society for Testing and Materials, 2001.